Eur. Phys. J. Appl. Phys. **80**, 30901 (2017)

https://doi.org/10.1051/epjap/2017170288

THE EUROPEAN PHYSICAL JOURNAL APPLIED PHYSICS

Regular Article

Flexible piezoelectric nanogenerators based on PVDF-TrFE nanofibers

Linda Serairi[1], Long Gu[2], Yong Qin[2], Yingxian Lu[3], Philippe Basset[3], and Yamin Leprince-Wang[1,*]

[1] Université Paris-Est, ESYCOM, UPEM, 5 bd. Descartes, 77454 Marne-la-Vallée, France
[2] Institute of Nanoscience and Nanotechnology, School of Physical Science and Technology, Lanzhou University, Lanzhou 730000, PR China
[3] Université Paris-Est, ESYCOM, ESIEE Paris, 2 bd. Blaise Pascal, 93162 Noisy-le-Grand, France

Received: 10 August 2017 / Received in final form: 14 November 2017 / Accepted: 27 November 2017

Abstract. In this paper, electrospun piezoelectric PVDF-TrFE nanofibers were used for the fabrication of two types of flexible nanogenerator (NG) devices based on the direct piezoelectric effect, allowing the conversion of mechanical energy into electrical energy. The first one is composed of quite well aligned thin film nanofibers of about 35 μm and the second one is composed of random nanofibers of about 50 μm. The influence of the applied stress and strain rate on the output for both types of NG was studied. It is shown that the pulse peaks generated by NG increase with the applied mechanical strain frequency, the generated output is also proportional to the applied stress amplitude. The first NG loaded in bending mode can generate a maximum voltage of 270 mV. By connecting two devices in series/parallel, the voltage/current value could be multiplied by two. The second NG which was biased in compression mode using a shaker controlled by a force sensor, can generate a potential of about 7 V under 3.6 N applied force.

1 Introduction

Recovery of environmental energy to power small electronic devices and systems, which is crucial for sustainable development, attracts the increasing attention since last decade [1,2]. Ambient energy is one of the most abundant and most popular energy in our daily life, which can range from wind energy to mechanical vibrations [3,4], ultrasonic waves [5], body motion and muscle stretching [6,7]. The recovery of these ambient energies received increasing attention due to the numerous potential applications in the development of microelectronics, self-powered systems, and wireless sensor networks [8–10].

Recently, inorganic materials (e.g. ZnO, InN, GaN) [11] have shown a remarkable ability to recover ambient energy with small mechanical forces. However, these inorganic materials are fragile and can be only operated in the very small stresses range.

Compared to the inorganic materials, ferroelectric polymers have attracted great interest in recent years for their application in energy harvesting due to their piezoelectric properties [12]. The ferroelectric polymers are flexible; thereby they are able to withstand greater mechanical deformation and greater stress, making them attractive for the ambient energy harvesting. As piezoelectric polymer, polyvinylidene fluoride (PVDF with $d_{33} \sim -20$ pC/N to -30 pC/N, $d_{31} \sim 20$ pC/N) and copolymer PVDF-TrFE ($d_{33} \sim -30$ pC/N to -40 pC/N, $d_{31} \sim 25$ pC/N) [13], are attractive materials in energy harvesting applications due to their low cost and large flexibility [14]. The piezoelectric property of PVDF and PVDF-TrFE has been used in various applications, such as hybrid nanogenerators (NGs) [15], piezoelectric transducers and NGs [13], etc.

PVDF is a semi-crystalline polymer, typically ∼50% crystalline, with four distinct crystal polymorphs named α, β, γ, and δ. This polymorph is directly related to the slightly larger van der Waals radius of fluorine (0.135 nm) versus hydrogen (0.12 nm) [16]. Except α-phase, all other three phases are polar version [17]. These different forms are fundamental to the unique properties and rich microstructure of PVDF and among the four polymorphs, the β-phase is most intriguing due to its piezo-, pyro- and ferroelectric properties. Thus, to get a better piezoelectricity of PVDF, the obtaining of the β-phase is necessary. This phase is conventionally obtained by stretching of the α-phase, or by crystallization from the polymer melt under high temperature and pressure (Fig. 1).

On the other hand, the PVDF-TrFE copolymer can be obtained in β-phase by adding a few quantity of TrFE in PVDF and annealing at temperature between T_c (Curie point) and T_m (melting point), with a higher crystallinity. The adoption of the copolymer PVDF-TrFE as functional material for flexible systems is more interesting due to its higher piezoelectric response than the PVDF and thus greater output electric power as energy harvesting material [18].

Although some piezoelectric NGs based on PVDF nanofibers have been reported using single nanofiber [19] or aligned PVDF nanofibers [20], obtained by near-field electrospinning (NFES) method, those piezoelectric NGs

* e-mail: yamin.leprince@u-pem.fr

on a flexible substrate had a low output voltage (<10 mV for stretch-release cycling frequency of 4 Hz). Liu et al. demonstrated the direct-write PVDF nonwoven fiber fabric energy harvesters via the hollow cylindrical NFES process having the output voltage peak of 74 mV at 7 Hz [21]. Chang et al. resumes some device designs based on PVDF and PZT nanofibers in their review paper on "Piezoelectric nanofibers for energy scavenging applications" [22].

In our design, we used the electrospun PVDF-TrFE nanofibers as active layer for the manufacture of two types of flexible NGs based on the direct piezoelectric effect in order to convert mechanical energy into electrical energy. The first NG device is based on well aligned fibers and the second one is based on random nanofibers. Both aligned and random fibers have been obtained by the far-field electrospinning process (higher efficiency than the NFES process, as most of the works reported in the literature). The output characterizations (voltage and current) have been carried out with different applied stress and strain rate on both types of NGs.

2 Design and fabrication

2.1 Electrospinning of PVDF-TrFE nanofibers

Figure 2 shows the experimental setup of conventional far-field electrospinning processes, which are more efficient than the near-field method [21,22]. The electrospinning solution was prepared following the method: a quantity of 1.3 g of PVDF-TrFE co-polymer powder (70:30, purchased from PIEZOTECH) was dissolved in a mixture of 3 mL of dimethylformamide (DMF, ACS reagent from VWR) and 7 mL of acetone (ACS reagent from VWR), and then the mixture has been heated at 60 °C for 30 min in order to obtain an homogeneous solution under magnetic stirring. The transparent viscous solution was transferred into a Hamilton syringe of 1 mL for the electrospinning use. A syringe pump (SP100i from WPI) and a high-voltage generator (LNC series, Heinzinger) are used for electrospinning rate control: a high voltage of 12 kV was applied between the syringe needle and the collector which was grounded; a distance of 10 cm was maintained between the needle and the collector. To obtain the aligned parallel nanofibers, the collector was a glass substrate on which a pair of copper electrodes with a gap of 2 cm was deposited (Fig. 2a). It is worth to note that the two copper electrodes were grounded together. For non-aligned fibers, a metal substrate has been used (Fig. 2b).

2.2 Fabrication of nanogenerator device

To obtain the NG based on the aligned PVDF-TrFE fibers, a piece of Kapton (dimension: 2 cm × 2.5 cm; thickness: 100 μm) was used as substrate. An interdigital gold electrode was fabricated on the Kapton substrate using the lithography technique (Fig. 3a), it is worth to mention that the width of each electrode is 400 μm and the distance between the electrodes is also 400 μm. The quite well aligned electrospun PVDF-TrFE fibers prepared on the glass substrate were carefully transferred over to the interdigital electrode (Fig. 3b). Several PVDF-TrFE layers have been superposed to form a polymer film of about 35 μm thick. After wire bonding on two electrodes, a PDMS layer of 500 μm has been deposited on the device for the dielectric protection (Fig. 3c).

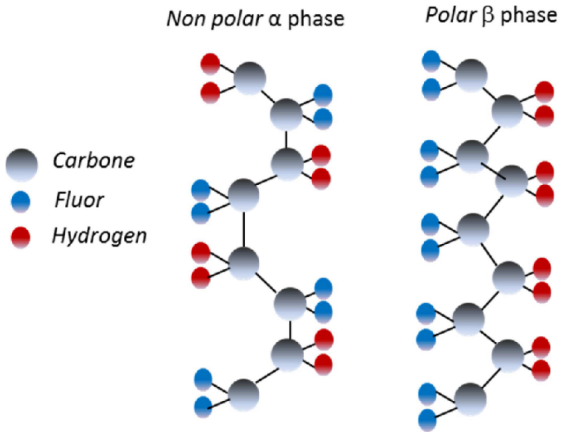

Fig. 1. Schematic diagrams showing crystalline structures of PVDF: non-polar α-phase and polar β-phase.

It is worth to highlight that the electric poling is necessary to align the PVDF-TrFE dipoles in the same direction which consists in applying a very high voltage to orientate the dipoles along the electrical field. Without poling, the local piezo effect will be cancelled at the macroscale. Thus, before test, the final device was biased at different voltages between 6 and 11 V/μm for one hour at the temperature of 100 °C, in order to align the PVDF-TrFE dipoles along the nanofiber direction by applying a electrical field on the two ends of the fibers.

Figure 3d shows a SEM image of the quite well aligned PVDF-TrFE nanofibers. In order to study the crystalline properties of the electrospun PVDF-TrFE fibers, the Fourier Transform Infrared spectroscopy (NEXUS 670) was performed. Figure 3e shows the main vibration peaks indicating the β-phase crystalline structure of the PVDF-TrFE [15].

To study the crystal structure of the nanofibers, we compared the microstructure of electrospun PVDF-TrFE nanofibers as deposited to the nanofibers post-annealed for 48 h at 135 °C. Figure 3f shows a comparison of XRD spectra of the fibers before and after annealing. In both cases, the peak on the diffraction pattern is centered on $2\theta = 20°$ indicating the piezoelectric β-phase of PVDF-TrFE. A slight crystallinity improvement of the microfibers PVDF-TrFE can be observed on the diffractogram which is indicating also the improvement of β-phase.

The polarity of the generated potential from the NG has been tested by forward connection and reversed connection to confirm the validity of the recorded piezoelectric responses.

3 Results and discussion

3.1 Nanogenerator based on the aligned PVDF-TrFE fibers

The working principle of the NG based on the aligned PVDF-TrFE nanofibers can be understood as follows. While applying an external compressive stress or tensile force (Fig. 3g), the fibers will act as a charge

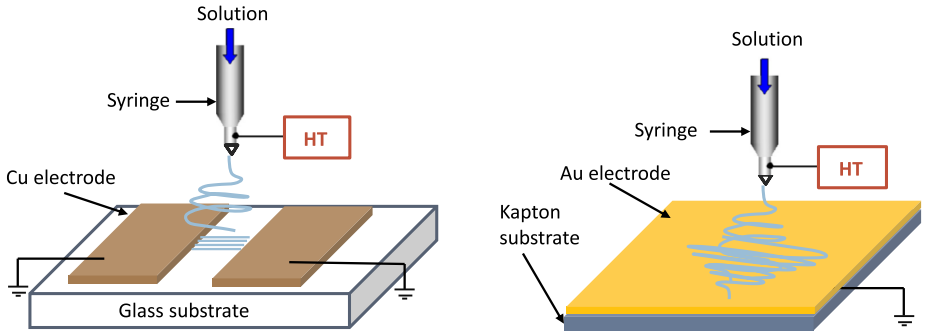

Fig. 2. Schema of electrospinning process: (a) to obtain the aligned fibers; (b) to obtain the random fibers.

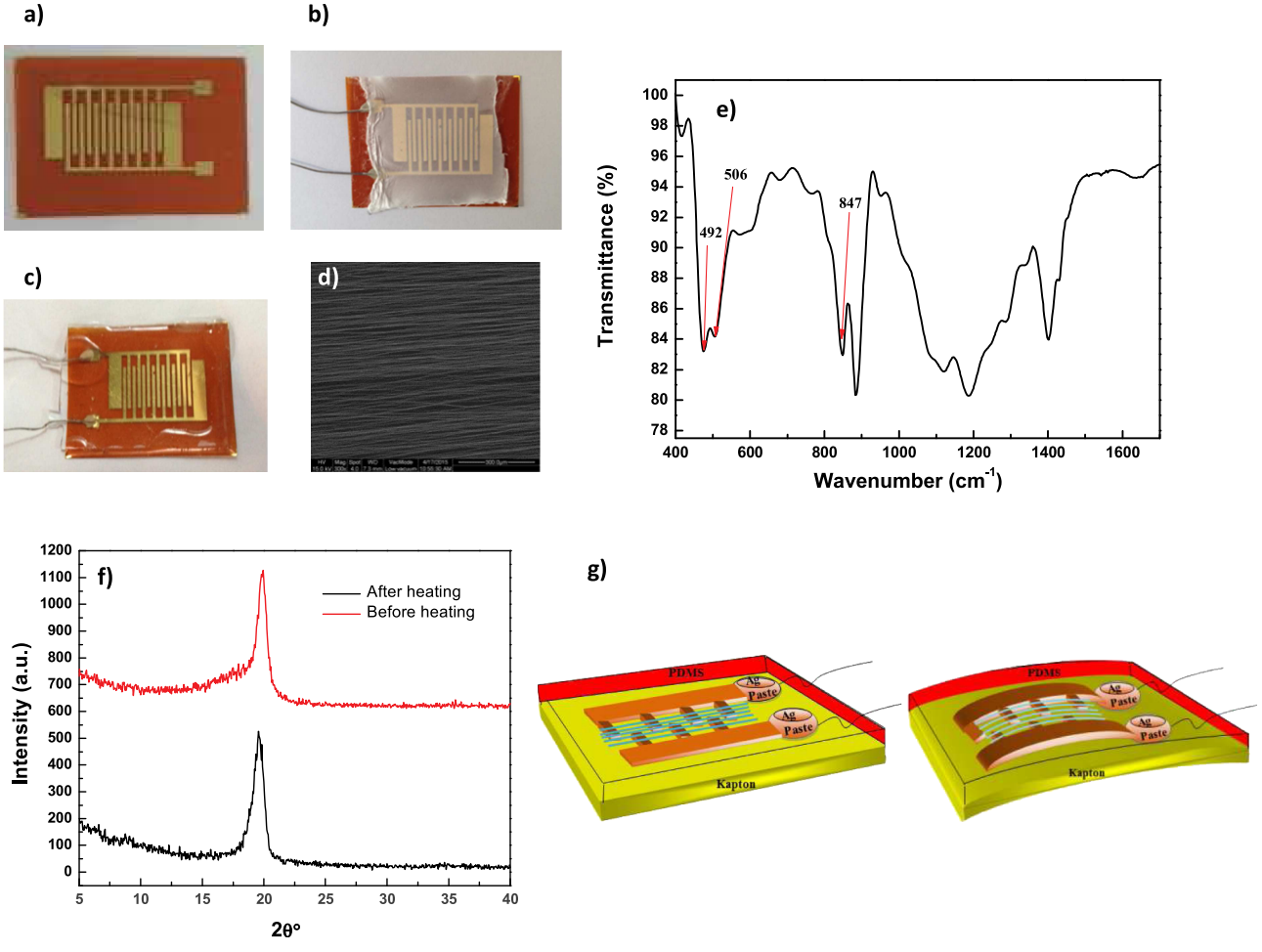

Fig. 3. (a) Au interdigitated electrode on Kapton substrate. (b) Deposition of aligned fiber. (c) Encapsulation of device with PDMS. (d) SEM image of well aligned PVDF-TrFE nanofibers. (e) FTIR transmission spectrum of electrospun PVDF-TrFE nanofibers. (f) XRD diffractogram of PVDF-TrFE nanofibers before and after annealing. (g) Schema of the NG device at rest and under mechanical bending which will create a tensile strain and a corresponding piezoelectric field along the fiber driving the electrons through an external circuit.

pump to drive electrons flow back and forth through the external circuit, which results in an alternating power source.

Figure 4a shows the sketch of strain action on the PVDF-TrFE fibers which is composed by 4 cycles: the linear motor does a positive movement to compress the flexible NG from t_0 to t_1 (cycle 1), it marks a break from t_1 to t_2 (cycle 2); and from t_2 to t_3 (cycle 3), the engine returns and releases the NG and finally, it marks a larger pause (t_3 to t_4, cycle 4) before moving to the second period. The motion and strain were controlled by a programmed linear motor (Fig. 4b).

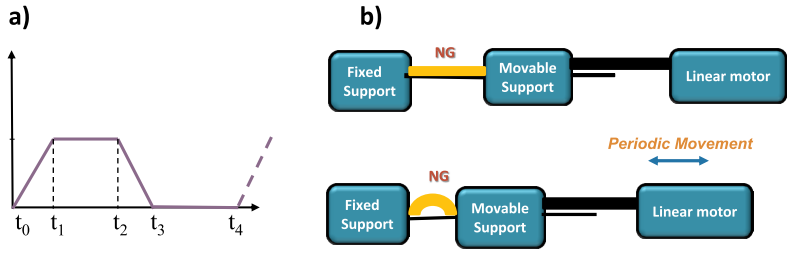

Fig. 4. (a) Schematic illustration of the period performed by the linear motor. (b) Schematic illustrating the movement of the linear motor: the sample is placed between two supports, the first is fixed and the second is movable and is controlled by the linear motor.

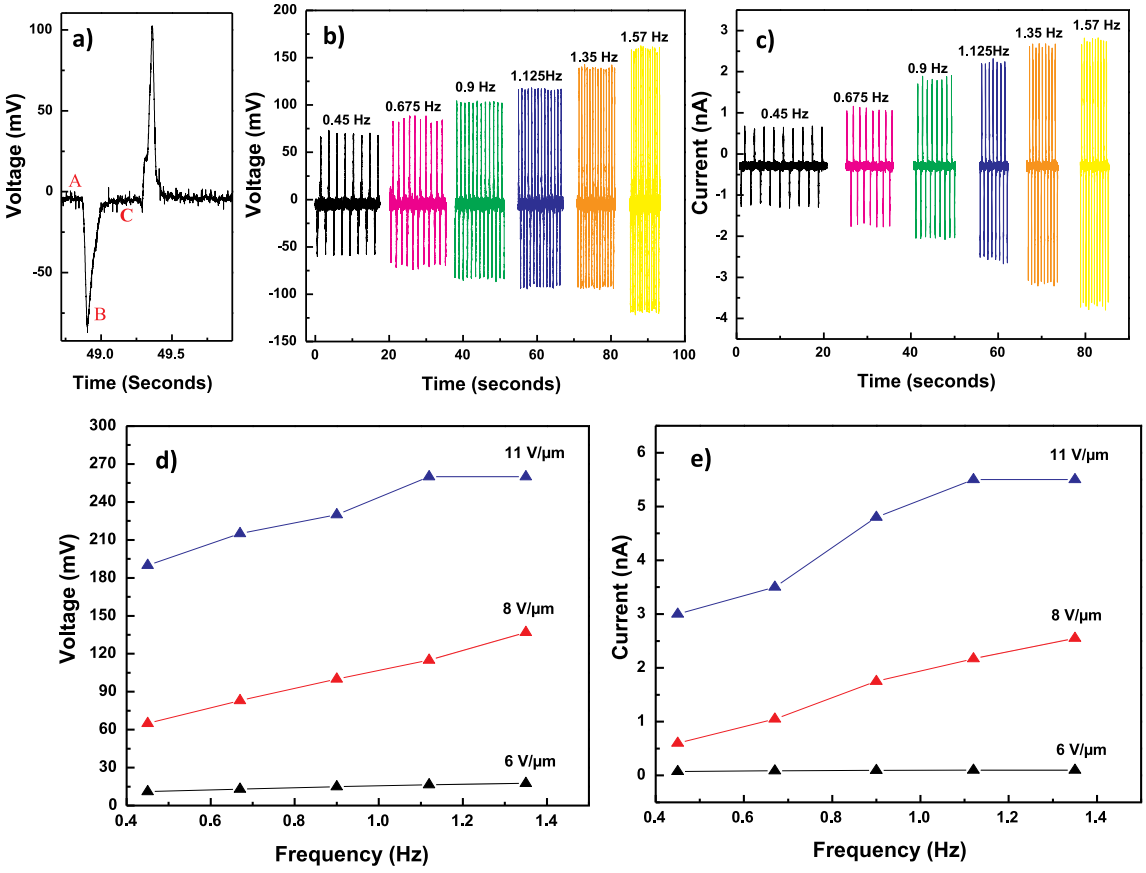

Fig. 5. Influence of the frequency on NG performance in bending test. (a) Enlargement of the NG voltage response. (b, c) The output voltage and output current of the NG for different stress frequencies ranging from 0.45 to 1.57 Hz with a polarization voltage of 8 V/μm. (d, e) Relationship between the peaks of the output voltage (output current) and the impact frequencies, under different electric field.

In this work, all voltage and current measurement have been carried out by using a low noise voltage preamplifier (SR560, Stanford Research Systems) with an internal resistance of 1 MΩ and a low noise current preamplifier (SR570, Stanford Research Systems) with an internal resistance of 100 MΩ. The complete experimental bench has been closed in a Faraday chamber in order to block the external electromagnetic field influence on the measurements. The current curve shown in Figure 5a increases from point A to point B with a negative slope and then decreases rapidly to zero (point C) corresponding to the cycle 1; after a short linear motor stop (cycle 2) during which the sample is released and some free charge in the external circuit is returning to the nanofibers surface by generating a positive pulse corresponding to cycle 3. A slight longer break of linear motor (cycle 4) completes the whole period in order to distinguish the step of cycle 4 from cycle 2.

The influence of the strain rate on the open loop voltage and the short circuit current produced by the PVDF-TrFE NG is shown in Figure 5b and c. The induced strain was fixed at 0.22% and has been applied at the frequency varying between 0.45 and 1.57 Hz. It is worth to note that the open circuit voltage increases from 15 to 20 mV and the short-circuit current increases from 0.2 to 0.3 nA while the strain rate is increasing from 0.45 to 1.57 Hz. This

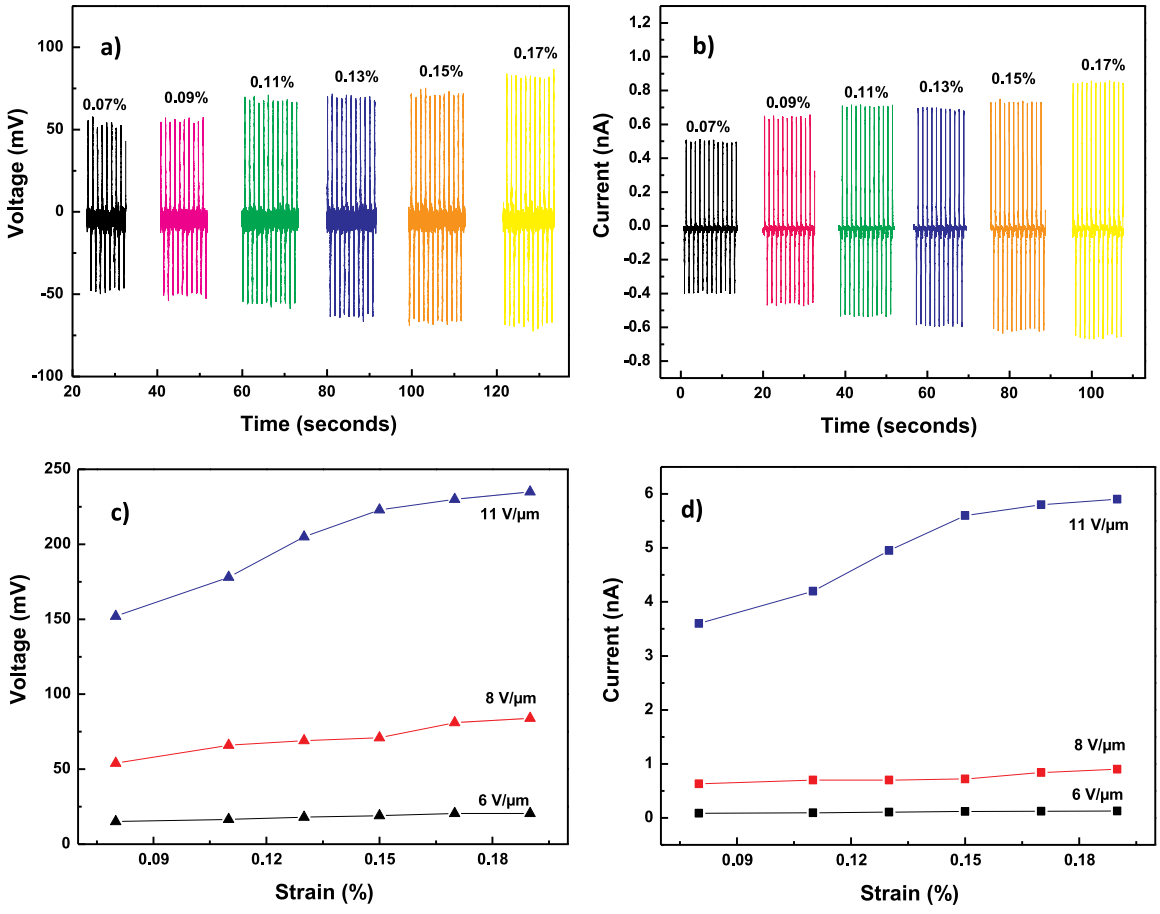

Fig. 6. Performance of the NG under different impact strains. (a, b) The output voltage and output current of the NG under different strains ranging from 0.07 to 0.17%, with a polarization voltage of 8 V/µm. (c, d) Relationship between the peaks of the output voltage (output current) and different strains for devices poled under different electric field.

observation is quite coherent with the piezoelectricity laws: the frequency increase will induce a shorter time to get the piezoelectric potential balance of the electrons in the external circuit, and this will lead to a higher current. As the external voltage is the product of the resistance and the external current, the voltage will increase correspondingly.

Figure 5d and e shows the evolution of voltage and current generated by the NG according to the frequency considering samples poled under strain rate under different applied electric fields ranging from 6 to 11 V/µm. It should be noted that the evolution of voltage/current is very weak for devices poled under 6 V/µm and 8 V/µm and it was increased noticeably from the poling field of 11 V/µm. This phenomenon could be explained by the fact that low bias applied on the PVDF-TrFE fibers is not enough to align all the dipole chains of PVDF-TrFE, which involves the cancellation of the local piezoelectric effect from certain dipoles leading to a decrease of piezoelectric performance of the NG at the macroscopic scale.

Secondly, to study the dependence of the applied stress on the output of NG, a various constraints ranging from 0.07 to 0.17% were applied on the device via amplitude controlled linear motor. The responses of the NG under various constraints are showed in Figure 6a and b, on which we can note that the generated current and voltage are proportional to the applied constraint. The relationship between the strain rate and the output peaks for devices poled under different applied electric fields is shown in Figure 6c and d. The measured potential and current increased with the applied constraint while the frequency was fixed at 0.9 Hz. We can also note that the higher polarization voltage, the higher generated voltage and current of the device.

In order to enhance the output performance, two NGs (with the active layer of about 35 µm and 25 µm, respectively) have been connected in serial and in parallel. The output voltage was approximately the sum of the output voltages of two individual NG when two NGs were connected in serial (Fig. 7a). The output current was approximately doubled when two NGs were connected in parallel (Fig. 7b). This demonstration means that the device output voltage and current can be modulated in the future by adding the NG unities connected in serial or in parallel according to the power need.

3.2 Nanogenerator based on the random PVDF-TrFE fibers

To prepare the random PVDF-TrFE nanofibers, we used the same electrospinning protocol previously described. In this case, the fibers were deposited directly on a Kapton substrate

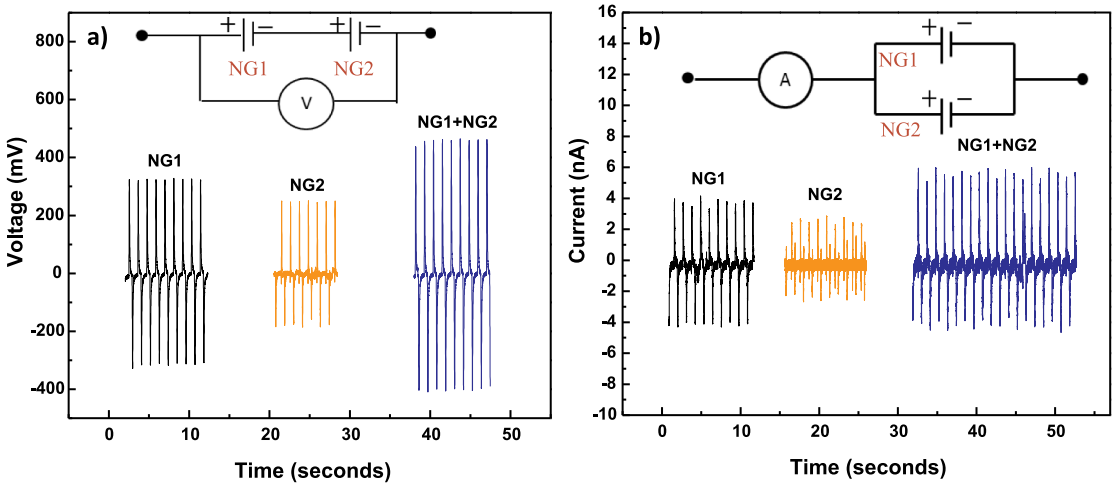

Fig. 7. Enhanced NG performance: (a) the output voltage of two nanogenerators connected in serial and (b) the output current of two nanogenerators connected in parallel.

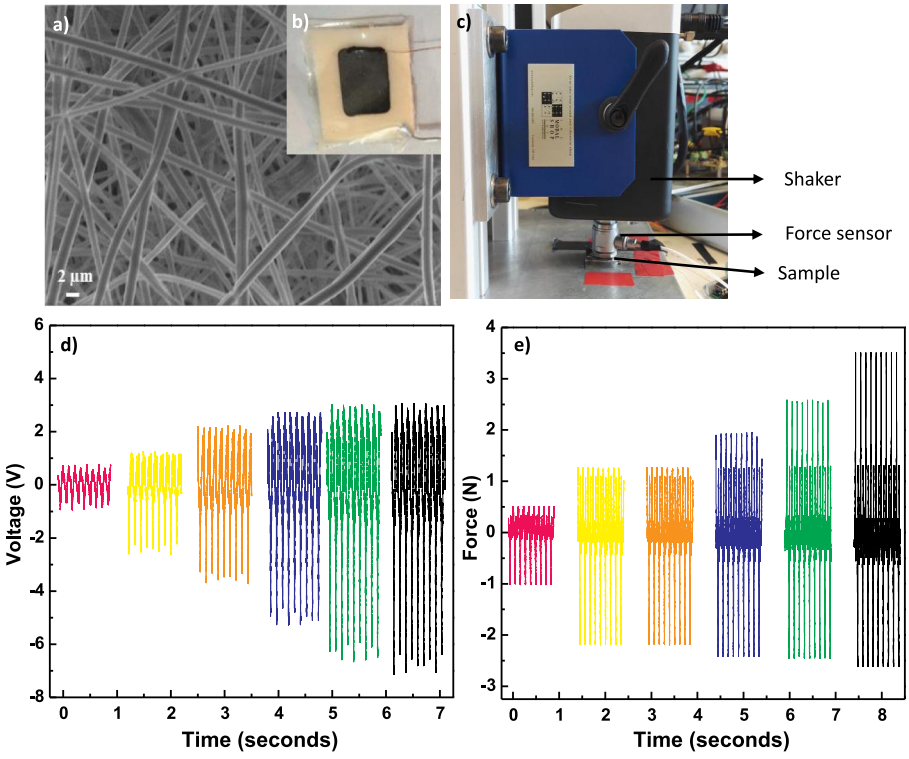

Fig. 8. Performance of the NG under different impact forces (with $f = 9$ Hz). (a) SEM image of PVDF-TrFE nanofibers showing their surface and structural morphology. (b) Optical image of PVDF-TrFE nanofiber based NG device. (c) Schematic of the used experimental setup. (d, e) The voltage output and applied force of the NG under impact exerted by a shaker.

covered with a gold film of about 500 nm as bottom electrode (see Fig. 2b). Figure 8a shows a SEM image of as deposited PVDF-TrFE random fibers. After electrospun fiber deposition (thick of about 50 µm), an aluminum top electrode of about 700 nm thickness was evaporated through a shadow mask. The final device was protected by a PDMS layer (Fig. 8b).

In this study, the NG was placed under a shaker (SmartShaker, Model K2004E01) applying a compressing force on the NG. The frequency was fixed at 9 Hz and the applied force was measured by a force sensor (DYTRAN MODEL 1053V2) (Fig. 8c).

Figure 8d shows the output voltage generated by the PVDF-TrFE nanofibers based NG, synchronized with the force applied by the actuator (Fig. 8e). The NG device withstood a large number of cycles (10 cycles for each curve performed) with a fixed frequency of 9 Hz and a maximal force was recorded at about 3.6 N. It should be noted that in this experiment the fibers are compressively stressed, thus generating a negative signal and an inverse signal will be generated when it is released. The profile of the generated signal therefore perfectly follows the profile of the force applied. A

maximum potential of 7 V has been obtained for an applied force of 3.6 N (Fig. 8d). It is a quite notable performance for this kind of NG.

4 Conclusion

In summary, the PVDF-TrFE electrospun nanofibers were synthesized to elaborate two types of NG devices: the first NG was based on the quite well aligned PVDF-TrFE fibers which worked in bending mode and can generate a maximum voltage of 270 mV and a current of about 5.5 nA for an active layer of about 35 μm; and the second NG was based on the random PVDF-TrFE fibers which worked in compression mode using a shaker. This NG with an active layer of about 50 μm, has a quite notable performance and can generate a potential up to 7 V with an applied force of 3.6 N. The electrical response (voltage and current output) depending on the applied external force has been systematically studied both on two types of NGs. The obtained measurements showed that the pulse peaks generated by NG increased with the applied mechanical strain frequency, and the generated output was also proportional to the applied stress amplitude. All those results are agreement with the piezoelectricity laws. It may be noted also that these NGs can be connected in series to increase the output voltage or in parallel to increase the output current; it will allow us to integrate number of devices according to the output power needs of many applications.

This work has been supported by the Ile-de-France region within the FUI 15 Program.

References

1. Z.L. Wang, *Nanogenerators for Self-Powered Devices and Systems* (Georgia Institute of Technology, SMARTech Digital Repository, 2011), http://hdl.handle.net/1853/39262
2. S.R. Anton, H.A. Sodano, Smart Mater. Struct. **16**, R1 (2007)
3. D. Wang, H. Ko, J. Micromech. Microeng. **20**, 025019 (2010)
4. H. Hneri, J. Sodano, J. Inman, Shock. Vib. Digest **36**, 197 (2004)
5. X. Wang, Y. Gao, Y. Wei, Z.L. Wang, Nano Res. **2**, 177 (2009)
6. J.E. Ferguson, A.D. Redish, Expert Rev. Med. Devices **8**, 427 (2011)
7. S. Samaun, K.D. Wise, E.D. Nielson, J.B. Angell, in Proceeding of Int Solid-State Circuits Conf, Digest of Tech. **104** (1971).
8. Y. Hu, Y. Zhang, C. Xu, L. Lin, R.L. Snyder, Z.L. Wang, Nano Lett. **11**, 2572 (2011)
9. S. Xu, B.J. Hansen, Z.L. Wang, Nat. Commun. **1**, 93 (2010)
10. S. Roundy, P.K. Wright, J. Rabaey, Comput. Commun. **26**, 1131 (2003)
11. X.D. Wang, J.H. Song, P. Li, J.H. Ryou, R.D. Dupuis, C.J. Summers, Z.L. Wang, J. Am. Chem. Soc. **127**, 7920 (2005)
12. Y. Liao, R. Wang, M. Tian, C. Qiu, A.G. Fane, J. Membr. Sci. 425–426, 30 (2013)
13. Z. Pia, J. Zhanga, C. Wena, Z.b. Zhang, D. Wu, Nano Energy **7**, 33 (2014)
14. D. Edmondson, S. Jana, D. Wood, C. Fang, M. Zhang, Analyst **138**, 7135 (2013)
15. S. Xu, B.J. Hansen, R. Yang, Z.L. Wang, ACS Nano **4**, 3647 (2010)
16. T. Yagi, M. Tatemoto, J.I. Sako, Polymer. J. **12**, 209 (1980)
17. M. Li, H.J. Wondergem, M.J. Spijkman, K. Asadi, I. Katsouras, P.W. Blom, D.M. de Leeuw, Nat. Mater. **12**, 433 (2013)
18. B.J. Chu, X. Zhou, K. Ren, B. Neese, M.R. Li, Q. Wang, F. Bauer, Q.M. Zhang, Science **313**, 334 (2006)
19. C. Chang, VH. Tran, J. Wang, Y.-K. Fuh, L. Lin, Nano Lett. **10**, 726 (2010)
20. J. Chang, L. Lin, IEEE Proc. Transducers **11**, 747 (2011)
21. Z.H. Liu, C.T. Pan, L.W. Lin, J.C. Huang, Z.Y. Ou, Smart Mater. Struct. **23**, 025003 (2014)
22. J. Chang, M. Dommer, C. Chang, L. Lin, Nano Energy **1**, 356 (2012)

Cite this article as: Linda Serairi, Long Gu, Yong Qin, Yingxian Lu, Philippe Basset, Yamin Leprince-Wang, Flexible piezoelectric nanogenerators based on PVDF-TrFE nanofibers, Eur. Phys. J. Appl. Phys. **80**, 30901 (2018)